ENVIRONMENTAL SCIENCE

Nonrainfall water origins and formation mechanisms

Kudzai Farai Kaseke,[1] Lixin Wang,[1]* Mary K. Seely[2,3]

Dryland ecosystems cover 40% of the total land surface on Earth and are defined broadly as zones where precipitation is considerably less than the potential evapotranspiration. Nonrainfall waters (for example, fog and dew) are the least-studied and least-characterized components of the hydrological cycle, although they supply critical amounts of water for dryland ecosystems. The sources of nonrainfall waters are largely unknown for most systems. In addition, most field and modeling studies tend to consider all nonrainfall inputs as a single category because of technical constraints, which hinders prediction of dryland responses to future warming conditions. This study uses multiple stable isotopes (^{2}H, ^{18}O, and ^{17}O) to show that fog and dew have multiple origins and that groundwater in drylands can be recycled via evapotranspiration and redistributed to the upper soil profile as nonrainfall water. Surprisingly, the non–ocean-derived (locally generated) fog accounts for more than half of the total fog events, suggesting a potential shift from advection-dominated fog to radiation-dominated fog in the fog zone of the Namib Desert. This shift will have implications on the flora and fauna distribution in this fog-dependent system. We also demonstrate that fog and dew can be differentiated on the basis of the dominant fractionation (equilibrium and kinetic) processes during their formation using the ^{17}O-^{18}O relationship. Our results are of great significance in an era of global climate change where the importance of nonrainfall water increases because rainfall is predicted to decline in many dryland ecosystems.

INTRODUCTION

Nonrainfall water (fog, dew, and vapor) is an important ecohydrological component of arid ecosystems (*1*, *2*) where any additional source of water may have a positive impact on productivity (*3*). However, nonrainfall water is less studied because research often focuses on factors limiting rather than sustaining productivity in arid environments. Hence, nonrainfall water is often not well characterized, and most ecological research tends to consider fog and dew inputs as one (*4*), although the two are derived from different meteorological phenomena.

For many coastal regions, the obvious source of fog and dew is the ocean (that is, advective fog and dew). However, many desert regions with reported nonrainfall water inputs have groundwater resources (*5*, *6*), which could be a source of nonrainfall water (that is, radiation fog and dew). It is often assumed that fog confined to river valleys in coastal deserts is advected inland from the ocean, but there is speculation that it may be generated locally as radiation fog (*7*). However, few studies address the sources of nonrainfall water, and as far as we are aware, no studies have investigated the possibility of groundwater contribution to nonrainfall water formation. How fog and dew will change in the future is dependent on their formation from their respective sources, ocean versus groundwater. Vegetation water use of both rainfall and nonrainfall components is essential for developing sound ecological models for arid environments (*8*) and key to understanding plant function under current or future climates (*9*). Differentiation of nonrainfall inputs will help build better ecological prediction models because the effect of global climate change on these ecosystems has not been adequately addressed (*10*).

Although stable isotopes ($\delta^{2}H$ and $\delta^{18}O$) have been applied widely to fog research (*11*), the application to dew research is minimal. To our knowledge, multiple stable isotope measurements have never been applied jointly to include both fog and dew within a given ecosystem. Because fog and dew involve condensation reactions, it is often assumed that their formation is similar to the liquid-vapor equilibrium state in clouds (*12*, *13*). The equilibrium assumption is likely true for fog formation (*14*); however, recent theoretical work suggests that dew formation could be dominated by kinetic fractionation processes (*15*). Because of the differences in fractionation processes, it is possible to differentiate fog and dew formation using the relationships of triple oxygen isotopes (^{16}O, ^{17}O, and ^{18}O) since a recent study shows that the $\delta^{17}O$-$\delta^{18}O$ slope is different for kinetic and equilibrium fractionation processes (*16*).

Like many dryland ecosystems worldwide, the Namib Desert is likely to experience changes in its hydrological cycle in response to global climate change (*17*, *18*). Given the abundance and importance of fog and dew in this desert (*19*), it provides an ideal location to study both components of nonrainfall water as part of the same ecosystem. Here, we collect diverse water samples (that is, rain, fog, dew, river water, and groundwater) and apply stable isotopes of hydrogen and oxygen ($\delta^{2}H$, $\delta^{17}O$, and $\delta^{18}O$) to differentiate fog from dew and determine source waters of these inputs in the Namib Desert at the Gobabeb Research and Training Centre (Fig. 1). These findings provide a new experimental framework to identify the origins of nonrainfall waters and differentiate fog and dew. These findings will assist in predicting dryland responses to global climate change by providing information about the sources of nonrainfall waters.

RESULTS

Isotopic characteristics of various waters

Rain, fog, dew, groundwater from two different depths, and Kuiseb River water were isotopically distinct, with rain being the most enriched in ^{2}H, ^{17}O, and ^{18}O compared to all other waters (Table 1). Trajectory analysis showed that rain events sampled during this period originated from the Atlantic Ocean (fig. S1); thus, isotopic enrichment of rain relative to all other waters (Table 1) is attributed to the "continental effect" and subcloud evaporation (note S1) (*12*, *20*, *21*). The ephemeral Kuiseb River water was depleted in ^{2}H, ^{17}O, and ^{18}O compared to local rainfall (Table 1), indicating that this water was sourced from headwaters at higher altitudes in the interior, and exhibited

[1]Department of Earth Sciences, Indiana University–Purdue University Indianapolis, Indianapolis, IN 46202, USA. [2]Desert Research Foundation of Namibia, 7 Rossini Street, Windhoek, Namibia. [3]Gobabeb Research and Training Centre, Walvis Bay, Namibia.
*Corresponding author. Email: lxwang@iupui.edu

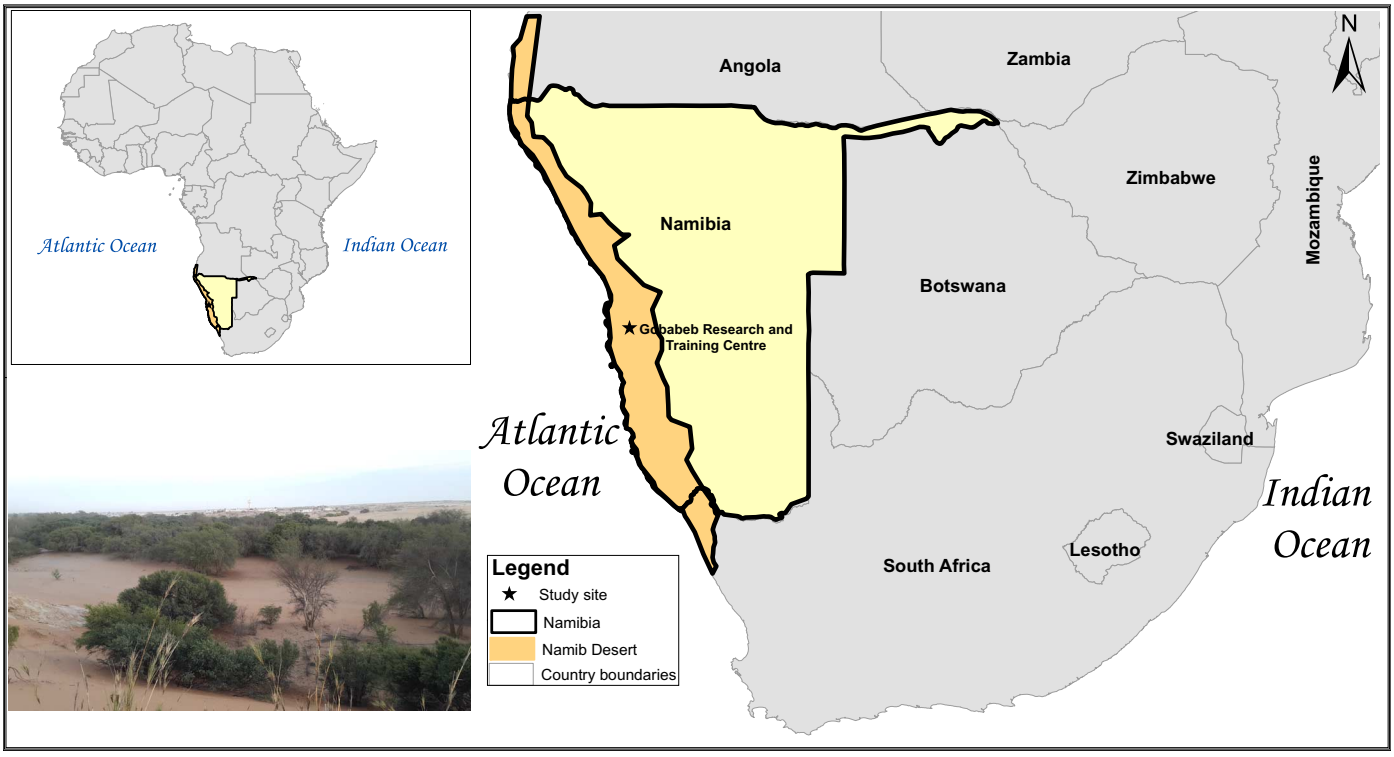

Fig. 1. Extent of the Namib Desert and location of the study site. The map shows the location of the Gobabeb Research and Training Centre and the extent of the Namib Desert, as well as an inset showing the general landscape characteristics around the study area: the Kuiseb River and the gravel plains. CREDIT: K.F.K./Indiana University–Purdue University Indianapolis.

Table 1. Isotopic characteristics (mean ± SD) of the various water samples at the Gobabeb Research and Training Centre, Central Namib Desert. Nonrainfall water refers to combined fog and dew samples. ‰, per mil; *n*, sample size.

Sample type	$\delta^{18}O$‰	$\delta^{2}H$‰	$\delta^{17}O$‰	*n*
Rain	+2.16 ± 3.0	+12.72 ± 28.84	+0.83 ± 2.9	5
Nonrainfall water	+0.39 ± 3.5	+3.74 ± 17.8	+0.11 ± 1.9	53
Dew (composite)	−1.25 ± 3.1	−7.97 ±13.7	−1.22 ± 1.6	15
Fog (composite)	+1.03 ± 3.4	+8.37 ± 17.3	+0.64 ± 1.8	38
River water (Kuiseb)	−11.49	−85.11	−6.51	1
Groundwater*	−9.33 ± 0.3	−63.97 ± 2.0	−4.54 ± 0.2	4
Groundwater†	−6.80 ± 0.2	−45.88 ± 0.7	−3.43 ± 0.2	2

*Shallow aquifer. †Deep aquifer.

an "altitude effect" (notes S1 and S2) (*22*). Nonrainfall water had large variability in all three isotopes, and when separated into fog and dew, these samples still exhibited large variability, suggesting the existence of different groups within these composite classes (Table 1).

Fog types and their origins

We identified three types of fog: advective, radiation, and mixed (see Materials and Methods and Fig. 2). There are no local open water sources close to the study site except the ephemeral Kuiseb River when in flow (note S1); thus, the only source of advective fog is the ocean. Fog formed from oceanic vapor is depleted in ^{18}O relative to ocean water (1 to 3‰; Fig. 2 and Table 2) (*23*). Furthermore, the isotopic composition of these samples (Table 2) was similar to those collected from the Namibian coast ($\delta^{18}O$, −0.86 to −0.39‰; $\delta^{2}H$, +0.80 to +3.30‰) (*7*). The Mann-Whitney *U* post hoc test showed that deuterium excess (d-excess) ($d = \delta^{2}H - 8.0 \times \delta^{18}O$) of advective fog (+7.2‰) was significantly lower than that of the global meteoric water line (GMWL) (+10‰) (Bonferroni-corrected $P < 0.05$), suggesting that evaporation at the source occurred at a relative humidity (RH) >85% or near equilibrium (*24*).

Advective fog is usually enriched in ^{2}H and ^{18}O compared to local rainfall (*25*), but our results show that advective fog was depleted in ^{2}H, ^{17}O, and ^{18}O compared to rainfall (Tables 1 and 2). Because of the close proximity of the study site to the Atlantic Ocean, both rain and advective fog could be considered first-stage condensates. However, whereas fog droplets remain at equilibrium with vapor, rain may experience subcloud evaporation due to aridity of the Namib Desert, resulting in enrichment of the rain compared to fog. This is supported by the low *d* exhibited by individual rain events (table S1) and the precipitation isoscape for Namibia (*21*).

Radiation fog *d* (−1.2‰) was significantly lower than advective fog *d* (+7.2‰) (Mann-Whitney *U* post hoc test, Bonferroni-corrected $P < 0.05$), which suggests that the two have different moisture sources since equilibrium fractionation does not change *d* (*20*). There was no significant difference between local meteoric water line (LMWL) *d* (−0.6‰) and radiation fog *d* (−1.2‰) (Table 2 and Fig. 1), suggesting that radiation fog was generated from local water sources (rainfall, ephemeral rivers, or shallow aquifers).

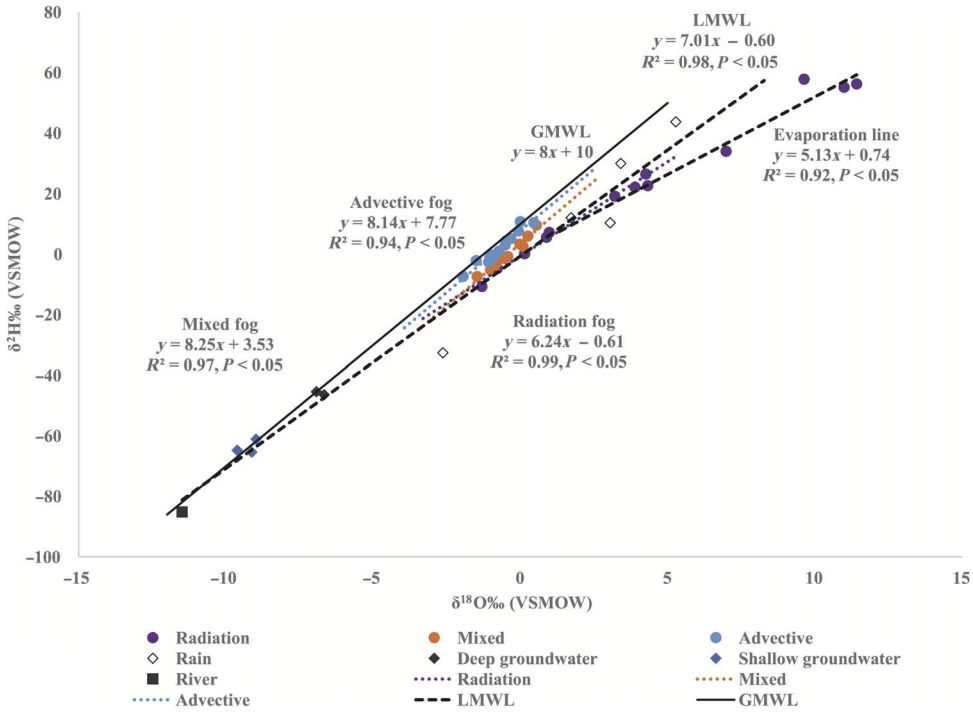

Fig. 2. Origins of fog water. The isotopic distribution of fog samples collected from the Gobabeb Research and Training Centre in relation to the GMWL and the LMWL, river water, and groundwater during the observation period (2014–2015). Fog regression lines indicate the source and classification of the fog. VSMOW, Vienna standard mean ocean water.

Table 2. Classification and isotopic characteristics (mean ± SD) of fog collected from the Gobabeb Research and Training Centre in the Namib Desert (2014–2015). *n*, sample size.

Classification	$\delta^{18}O$‰	$\delta^{2}H$‰	$\delta^{17}O$‰	*d*‰	*n*
Advective	−0.74 ± 0.6	+1.76 ± 5.1	−0.20 ± 0.5	+7.67 ± 1.3	15
Mixed	−0.43 ± 0.6	+0.01 ± 5.3	−0.23 ± 0.5	+3.42 ± 1.0	10
Radiation	+1.41 ± 2.1	+8.18 ± 13.3	+0.78 ± 1.1	−2.24 ± 3.4	8

Mixed fog *d* (+3.2‰) was significantly higher than LMWL *d* (−0.6‰) but significantly lower than advective fog *d* (+7.2‰) (Mann-Whitney *U* post hoc test, Bonferroni-corrected $P < 0.05$) (Fig. 1 and Table 2), providing evidence of the mixing of different air masses to generate fog (*26*, *27*). There were no significant differences in all three isotopes ($\delta^{18}O$, $\delta^{2}H$, and $\delta^{17}O$) between mixed fog and either advective or radiation fog, suggesting that mixed fog retains characteristics of both moisture sources (Fig. 2). However, radiation fog ^{18}O (+0.98‰) and ^{17}O (+1.08‰) were significantly enriched compared to advective fog ^{18}O (−0.94‰) and ^{17}O (+1.08‰) (Mann-Whitney *U* post hoc test, Bonferroni-corrected $P < 0.05$; Table 2). Figure 2 shows two clusters of radiation fog on the LMWL: rain-derived ($\delta^{18}O$, +3.78 ± 0.5‰; $\delta^{2}H$, +22.6 ± 3.72‰; $\delta^{17}O$, +1.75 ± 0.6‰) (*28*) and groundwater-derived ($\delta^{18}O$, −0.02 ± 1.0‰; $\delta^{2}H$, −0.48 ± 7.4‰; $\delta^{17}O$, +0.20 ± 0.9‰) (see Materials and Methods).

Dew types and their origins

We identified three types of dew: groundwater-derived, advective, and shallow soil water–derived dew (see Fig. 3 and Materials and Methods). The calculated source isotopic composition of groundwater-derived dew ($\delta^{18}O$, +0.35‰; $\delta^{2}H$, +1.84‰) and groundwater-derived fog ($\delta^{18}O$, −0.02 ± 1.0‰; $\delta^{2}H$, −0.48 ± 7.4‰) were similar and can be viewed as evidence that the two have the same origin (see Materials and Methods). Wen *et al.* (*29*) demonstrate theoretically that dew formation under supersaturated conditions is controlled by kinetic fractionation processes, but detection using $\delta^{2}H$ and $\delta^{18}O$ is difficult. We did not find any significant differences in both $\delta^{18}O$ and $\delta^{2}H$ between groundwater-derived dew ($\delta^{18}O$, −2.32‰; $\delta^{2}H$, −12.33‰) and groundwater-derived radiation fog ($\delta^{18}O$, +0.14‰; $\delta^{2}H$, −12.33‰) (Kruskal-Wallis test, $P > 0.05$). However, groundwater-derived dew ^{17}O (−1.86‰) was significantly depleted compared to groundwater radiation fog ^{17}O (+0.39‰) (Mann-Whitney *U* post hoc test, Bonferroni-corrected $P < 0.05$), suggesting that $\delta^{17}O$ could be the key to differentiation of fog and dew isotopically. Groundwater-derived dew *d* (+6.21‰) was significantly higher than both the LMWL *d* (−0.6‰) and groundwater-derived radiation fog *d* (−0.6‰) (Mann-Whitney *U* post hoc test, Bonferroni-corrected $P < 0.05$) (Fig. 3B and Table 3). Because groundwater has an inherently low *d*, the unusually high *d* of groundwater-derived dew suggests strong kinetic fractionation processes during its formation similar to that reported for liquid condensation (*15*).

The calculated source isotopic composition of advective dew ($\delta^{18}O$, −0.56‰; $\delta^{2}H$, +5.53‰) was similar to that of advective fog, indicating similar origins (see Materials and Methods and Table 2). The *d* value of advective dew (+16.0‰) is much higher than expected (Table 3) and is likely influenced by kinetic fractionation processes during two stages: evaporation of moisture from the ocean and condensation. This combined kinetic isotope effect could thus account for the unusually large *d* (Table 3). The isotopic composition of source water and the advective dew line (Fig. 3B) are similar to those reported for the Negev desert ($\delta^{18}O$, −0.68‰; $\delta^{2}H$, +4.54‰; $\delta^{2}H = 3.9 \times$

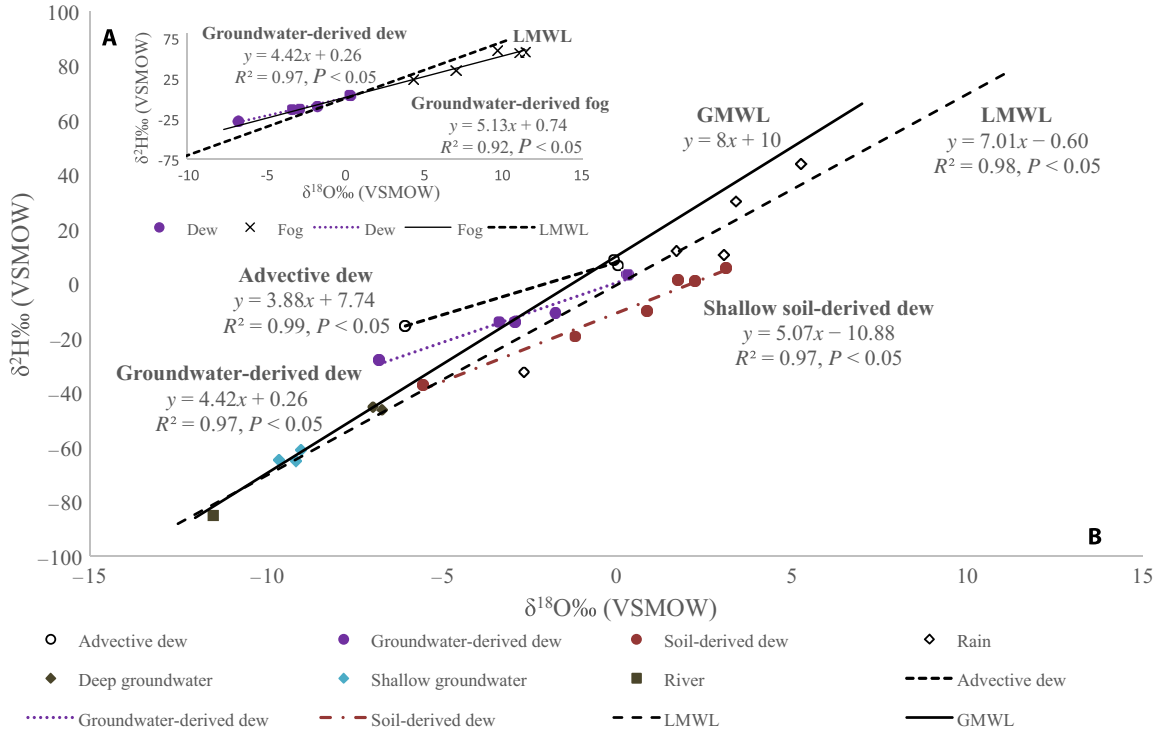

Fig. 3. Origins of dew water. (**A**) Groundwater-derived dew and fog lines indicating similar origins and plotting along the same evaporation line. (**B**) The LMWL at the Gobabeb Research and Training Centre with groundwater, Kuiseb River water, rain, and dew isotopes collected from 2014 to 2015. The GMWL was included as a reference.

Table 3. Isotopic characteristics (mean ± SD) and classification of dew samples from the Gobabeb Research and Training Centre in the Namib Desert (2014–2015). *n*, is sample size.

Dew classification	$\delta^{18}O$‰	$\delta^{2}H$‰	$\delta^{17}O$‰	*d*‰	*n*
Advective	−2.01 ± 3.5	−0.07 ± 13.5	−1.77 ± 1.7	16.0±14.3	3
Groundwater-derived	−2.35 ± 2.7	−10.12 ± 11.9	−1.75 ± 1.4	8.67±9.7	6

$\delta^{18}O$ + 7.2) (*30*), suggesting that this could be universal for advective dew from the ocean. The isotopic composition of shallow water–derived dew ($\delta^{18}O$, −5.30‰; $\delta^{2}H$, −37.75‰) does not match any of the water sources identified for the ecosystem (Table 1) but was likely formed from evaporative discharge from the shallow alluvial aquifer (see Materials and Methods and Fig. 3) (*31*).

Separation of fog and dew

The $\delta'^{17}O$-$\delta'^{18}O$ slope of bulk fog samples (that is, combining all fog types; see Materials and Methods) was 0.528 (Fig. 4), indicating that meteoric waters condensed under isotopic equilibrium (*16*, *32*). This agrees with previous conclusions on advective and radiation fogs based on interpretations of *d* and the calculated fractionation factors (see Materials and Methods). Therefore, the isotopic composition of fog is determined by equilibrium fractionation processes regardless of fog type. The $\delta'^{17}O$-$\delta'^{18}O$ slope of bulk dew samples (that is, combining all dew types; see Materials and Methods) was 0.516 (Fig. 4), indicating that dew formation is dominated by kinetic fractionation processes (*16*) regardless of its origin. Kinetic fractionation during the vapor-liquid phase change is related to the degree of supersaturation and differences in diffusive velocities of isotopic molecular species through supersaturated air (*15*) similar to the vapor-solid phase change (*33*, *34*). This is the first reported field evidence of kinetic fractionation dominating the oxygen isotope composition of dew during natural formation. We found no significant differences between $\delta^{18}O$ values in bulk fog (−0.38‰) and bulk dew (−0.07‰), as well as *d* values in bulk fog (+3.75‰) and bulk dew (+3.17‰) (Kruskal-Wallis test, $P > 0.05$). However, fog ^{2}H (+2.82‰) and ^{17}O (+0.08‰) were significantly enriched compared to dew ^{2}H (−10.06‰) and ^{17}O (−0.09‰) (Mann-Whitney *U* post hoc test, Bonferroni-corrected $P < 0.05$).

DISCUSSION

Identification of the origins of fog and dew, particularly in arid ecosystems, by their stable oxygen and hydrogen isotopic compositions will permit future studies to ascertain the response of these ecosystems to increased warming and global climate change. Here, we used $\delta^{18}O$ and $\delta^{2}H$ values, and the corresponding positions on the LMWL and GMWL (Figs. 2 and 3), to demonstrate the origins of fog and dew. The LMWL of a hyperarid environment, such as the Namib Desert, should have a slope <8 due to the strong atmospheric demand. Inclusion of advective and mixed fog samples in the meteoric water line could result in an LMWL with a slope ≥8 because advected fog is not derived from local meteoric water (Fig. 2). Therefore, fog should be excluded from the determination of LMWL. The isotopic classification of dew and fog was verified using *d* values. We also provided wind direction and wind speed measurements from the study site, and

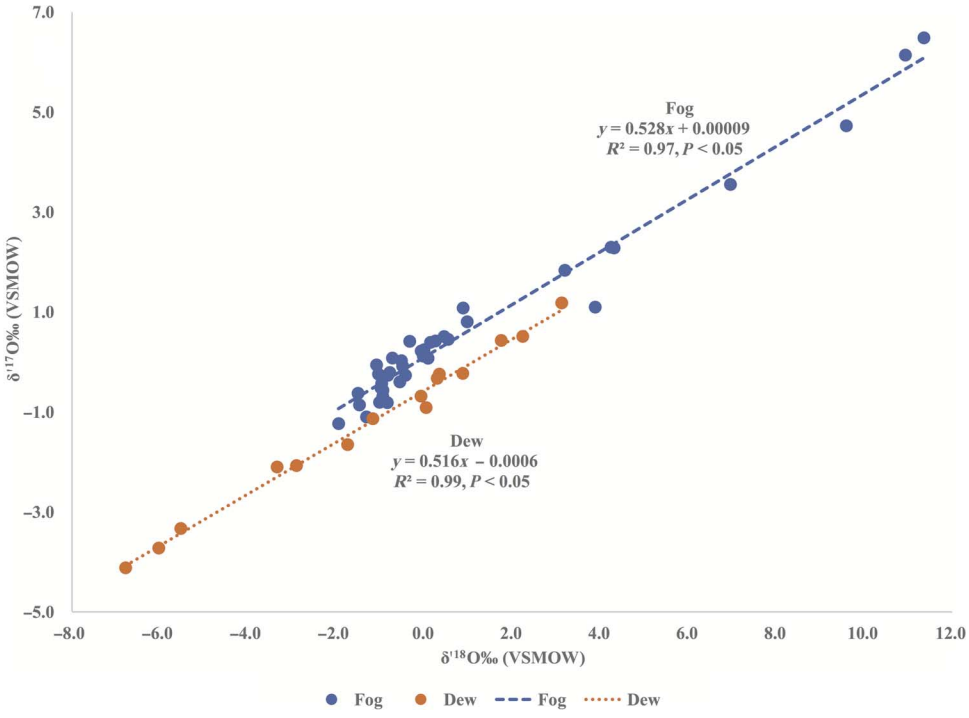

Fig. 4. Differentiation of fog and dew. $\delta'^{17}O$ versus $\delta'^{18}O$ plots for bulk fog and dew samples showing that fog and dew are controlled by different fractionation processes: equilibrium and kinetic, respectively.

they are generally consistent with our classifications (note S3 and table S2). For example, advective and mixed fogs have westerly origins from the Atlantic Ocean, whereas radiation fog originates from a southerly direction consistent with the position of the Kuiseb River at the study site. Wind speeds accompanying advective fog are higher than those of mixed and radiation fogs (table S2 and note S3). Furthermore, we verified groundwater as the source for groundwater-derived fog using theoretical fractionation factor calculations (see Materials and Methods). We acknowledge that direct isotopic measurements of transpiration vapor would strengthen our estimates of the fractionation factors (see Materials and Methods). However, these measurements would not change our conclusions. We also note that recent spectroscopy-based transpiration studies have shown that the isotopic composition of transpiration vapor closely approximates its source waters (*35*, *36*), supporting the assumption that we made in our fractionation factor calculations (see Materials and Methods). In addition, we believe that the coherent multiple lines of evidence provided here (for example, positions on isotopic water lines, theoretical fractionation factor calculations, wind speed/direction, and *d* values) provide strong support for our estimates of the source origins of fog and dew.

On the basis of our estimated source origins of fog and dew, groundwater in alluvial aquifers may have a much larger impact than often acknowledged in arid environments. Groundwater is evapotranspired through riparian vegetation, forming radiation fog and/or dew, and is redistributed into the upper few centimeters of the soil profile, making it available for use by other life forms. Esler *et al.* (*37*) postulate that the ecophysiology of prostrate-leaved geophytes in arid environments enhances dew formation by lowering leaf temperature. On the other hand, *Stipagrostis sabulicola* is adapted for efficient fog harvesting because of its surface traits and upright structure (*38*, *39*). Therefore, nonrainfall waters have important implications on species survival and distribution.

On the basis of our analyses, radiation fog was the dominant fog type at the study site during the study period. From the samples collected, the frequency of each fog type was as follows: 39.5% for advective fog, 34.2% for radiation fog, and 26.3% for mixed fog. However, mixed fog could be considered as a form of radiation fog because it is generated by radiative cooling and localized radiation fog thus accounted for 60.5% of the fog occurrence during this period. This result is surprising because the study site lies on the edge of the Namib fog zone and is thought to be influenced more by advective fog. Our results suggest that advective fog is dissipating closer to the coast than the 60-km inland boundary used to define the fog zone. There is further corroborative evidence from our site that shows a receding range in the occurrence of fog-harvesting beetles to less than 60 km inland. Increasing global air temperatures would increase soil temperatures and result in a 0 to 20% decline in RH and decrease in cloud immersion in cloud forests (*40*). Although not a cloud forest, the principle is applicable to the Namib fog zone and could be evidence that global climate change is diminishing this fog zone. If true, we expect to observe more changes in the flora and fauna composition over the outer edge of the Namib Desert fog zone. This is because radiation fog is spatially variable and its dominance is related to a decrease in advective fog rather than an increase in frequency of radiation fog. Consequently, fog input to the area is decreasing, with fog frequency dropping 56% from 2001 (*19*) to the time of this study. In addition, radiation fog is confined to topographic lows and ephemeral channels (*7*), although behavioral adaptations of fauna (for example, fog-harvesting beetles) show that they position themselves on dune crests to harvest fog. This advective-radiation fog shift may necessitate redefining the extent of the Namib fog zone and provide an opportunity to study the effects of global climate change on fog-dependent systems.

Because of technical constraints, most previous research tends to treat dew inputs as fog (*4*) or vice versa in dewy deserts such as the

Negev, where fogs are often regarded as dew (*41*). Our results demonstrate that fog and dew are dominated by different fractionation processes, equilibrium and kinetic, respectively, and this can be used as a basis for differentiation of the two inputs using the ^{17}O-^{18}O relationship. The new ^{17}O-^{18}O method developed here to differentiate fog and dew will thus enhance the understanding of vegetation water-use strategies in nonrainfall water–dependent ecosystems. By determining the significance of each nonrainfall water input to specific plant species, we could more accurately model the climate change impact on plant species and fauna that depend on it.

MATERIALS AND METHODS

Isotope analysis

Sample collection was described in detail in the Supplementary Materials (note S2). We used a Triple Water Vapor Analyzer (Los Gatos Research Inc.) for isotopic analysis with a precision of 0.2‰ for $\delta^{18}O$, 0.8‰ for $\delta^{2}H$, and 0.4‰ for $\delta^{17}O$, similar to those reported elsewhere (*42*, *43*). Data were reported in δ notation relative to VSMOW–Standard Light Antarctic Precipitation (SLAP) scale as

$$\delta = \frac{R_{sample}}{R_{VSMOW}} - 1 \quad (1)$$

where R_{sample} and R_{VSMOW} are the molar ratios of heavy to light isotopes ($^{2}H/H$, $^{18}O/^{16}O$, or $^{17}O/^{16}O$) of the sample and international standard (VSMOW). However, it has been demonstrated that when dealing with high-precision ratios in multiple systems, a modified δ is preferred (*44*–*46*), hereafter designated as δ′ and defined as

$$\delta'^{*}O = \ln(\delta + 1) = \ln\frac{R_{sample}}{R_{VSMOW}} \quad (2)$$

where *O is either ^{17}O or ^{18}O.

Differentiation of nonrainfall vectors based on isotopes

During the period of sampling (2014–2015), we analyzed a total of 65 water samples (38 for fog, 15 for dew, 5 for rain, 6 for groundwater, and 1 for river water) (tables S1 and S2). Monthly rainfall data between 2013 and 2015 were also provided in table S3, which was from Lu *et al.* (*47*). Oxygen and hydrogen isotope analysis of these samples permitted us to differentiate three basic types of fog: advective, radiation, and mixed (that is, fog source water derived from both ocean and local waters). Differentiation of fog type was based on the knowledge that fog is a first-stage condensate controlled by equilibrium fractionation processes and plots on a meteoric water line, reflecting its origins (*12*, *13*, *48*). Because the Namib fog zone is characterized by advective fog originating from the Atlantic Ocean and the sampling location is close to the ocean (~60 km) (*49*), we expect advective fog to plot on the GMWL (Fig. 2). We expect that locally generated (radiation) fog should plot on the LMWL, reflecting local meteoric water origins (Fig. 2). The LMWL for this site was defined on the basis of groundwater and rain samples, excluding fog from its determination (Fig. 2). The LMWL had a smaller slope and lower intercept than the GMWL, indicating evaporative enrichment of local waters, a characteristic of arid environments (Fig. 2). Our LMWL was similar to that defined as $\delta^{2}H = 7.2 \times \delta^{18}O - 0.6‰$ (*31*), although that LMWL included fog in its definition. As advective fog dissipates downwind in the Namib, it persists as a high-humidity air mass (*50*), which mixes with local moisture from the vicinity of the study site. Radiative cooling of this mixed air then results in mixed (advective-radiation) fog, which retains characteristics of both moisture sources and plots between the GMWL and the LMWL (Fig. 2). We used *d* to verify the source of fog apart from how it plots relative to the meteoric water lines.

Groundwater has two distinct isotope signatures that indicate the existence of two alluvial aquifers at the study site (Table 1). Both are likely dependent on recharge through the ephemeral riverbed (*51*) via short-duration water flow (*52*). Figure 2 shows two clusters of radiation fog: One cluster plots among the rain samples indicating local rainfall origins (*28*), and the second cluster plots below the rain samples eliminating local precipitation as the source origin (table S2 and fig. S1). This fog cluster occurred when the river was dry, suggesting groundwater as the possible origin, hence classified as groundwater-derived radiation fog (Fig. 2). Radiation fog (Table 2) is thus a composite of fog derived from local water sources, each with a unique isotopic signature reflecting the source water (Fig. 2).

To verify groundwater as the source for groundwater-derived fog (Fig. 2), we presented theoretical calculations based on isotope principles. It is estimated that 48 to 80% of local rainfall in tropical regions is from recycling of water to the atmosphere via evapotranspiration (*53*, *54*), with transpiration being the largest component of the evapotranspiration flux (*55*, *56*). Transpiration is nonfractionating. Therefore, transpired water vapor is isotopically similar to xylem water (*57*) and reflects the isotopic signature of the source water used (*58*). Because the isotopic composition of fog is related to equilibrium with atmospheric vapor, similar to the liquid-vapor equilibrium state found in clouds (*12*, *13*), we assumed that the fog condensate is at equilibrium with transpired vapor and that transpired vapor reflects the groundwater isotopic signature. In support of these assumptions, recent spectroscopy-based transpiration studies have shown that the isotopic composition of transpiration vapor is similar to that of the source waters (*35*, *36*)

$$\alpha_{l-v} = \frac{1000 + \delta_l}{1000 + \delta_v} \quad (3)$$

where δ_l is isotopic composition of the fog condensate and δ_v is the isotopic composition of the transpired vapor, which reflects the groundwater isotopic composition (Table 1).

Using the average isotopic composition of the groundwater-derived fog ($\delta^{18}O$, −0.02‰; $\delta^{2}H$, −0.48‰) and applying the groundwater isotopic compositions from Table 1 to Eq. 3, we obtained $^{18}\alpha_{l-v} = 1.0094$ and $^{2}\alpha_{l-v} = 1.0678$ for shallow groundwater and $^{18}\alpha_{l-v} = 1.0068$ and $^{2}\alpha_{l-v} = 1.0478$ for deep groundwater. The fractionation factors obtained using the shallow groundwater were similar to the equilibrium fractionation factors at 20°C (1.0098 for $\delta^{18}O$ and 1.084 for $\delta^{2}H$) determined from experimental work (*48*). We further estimated the RH condition during fog formation based on the observed fractionation factors. We assumed that equilibrium fractionation occurs at 100% RH for the experimental work (*48*) and then $^{2}\alpha/^{18}\alpha$ = 84‰/9.8‰ = 8.57. Combining this information and our calculated fractionation factors, RH during fog formation in our study was (67.8‰/9.4‰)/8.57 = 84.2%, which was within the range of observed RH for fog events at this site (*50*). Furthermore, a previous study showed that most ephemeral vegetation in the lower Kuiseb is reliant on the shallow aquifer depending on stage of growth and species (*31*). These

multiple lines of evidence supported the classification of groundwater-derived fog.

Similar to fog, dew can be classified on the basis of their positions relative to the GMWL and LMWL. In any ecosystem, dew has at least three sources: lower atmosphere, shallow soil layer, and deep soil layer/groundwater (*29*). During evaporative enrichment of water, vapor will have a reciprocal depletion and plot on the same evaporative line but opposite the initial composition of water (that is, left of the meteoric water line). Condensation of this vapor on a sufficiently cooled substrate surface results in dew and, in theory, should plot along the evaporative line but to the left of the relevant meteoric water line. On the basis of this theory, we can classify dew by calculating the isotopic composition of the dew source and comparing it to the isotopic signatures of the different pools of water to identify its origins (Table 1 and Fig. 3). Extending the evaporation line of groundwater-derived radiation fog beyond the LMWL, we observed that dew samples plot along this line, suggesting similar origins (Fig. 3, A and B). Advective dew plotted to the left of the GMWL and its source isotopic composition was similar to that of advective fog derived from the ocean, suggesting similar origins (Fig. 3B and Table 2). The source isotopic signature of dew derived from shallow soil did not resemble any of the isotope compositions in Table 1. However, $\delta^{18}O$ was similar to that indicated for soil at 0.5 m depth in the Kuiseb River in a $\delta^{18}O$ versus depth profile (*31*). Unfortunately, $\delta^{2}H$ was not reported. Therefore, we applied the LMWL defined in this study to calculate $\delta^{2}H$ (37.81‰), which is similar to our calculated source water value. Our data suggest that this dew was derived from shallow soil water at about 0.5 m. We did not characterize the isotopic signatures of the dew derived from shallow soil because most of these samples plotted to the right of both meteoric water lines, which suggests that they have undergone evaporative enrichment (Fig. 3B).

Of the 38 fog samples, 5 showed evidence of evaporative enrichment (Fig. 2). However, because all the samples were handled in the same manner, this enrichment could be formation-induced. We excluded these five fog samples from isotope characterization but calculated their source isotope composition ($\delta^{18}O$, +0.71‰; $\delta^{2}H$, +4.40‰), which is similar to that of the groundwater-derived fog. Hence, they were classified as radiation fog (groundwater-derived). Because the enrichment could be formation-induced, we included these samples into the bulk fog classification for $\delta'^{17}O$ versus $\delta'^{18}O$ analysis. Similarly, most of the soil-derived dew samples plotted to the right of the LMWL, suggesting evaporative enrichment; thus, we did not isotopically characterize this dew type. Because of the differences in fractionation processes in fog (equilibrium-dominated) and dew (kinetic-dominated), we used the $\delta'^{17}O$ versus $\delta'^{18}O$ relationship to differentiate fog and dew (Fig. 4).

Statistical analyses

All statistical analyses were performed using nonparametric methods in PAST 3 (Paleontological Statistics, Natural History Museum, University of Oslo), the Kruskal-Wallis test, followed by a Mann-Whitney *U* post hoc test with $P = 0.05$ for significance. Because advective and radiation fog were derived from different meteoric waters, we compared each fog to its respective meteoric water line (for example, *d* of advective fog was compared to that of the GMWL, whereas *d* of radiation fog was compared to that of the LMWL) (Fig. 2). Using the *d* of advective fog, we can determine the evaporation conditions over the ocean, and if significantly greater than that of the GMWL, we can conclude that evaporation occurred under low humidity (RH, <85%) (*59*). If the *d* of the generated radiation fog is significantly greater than that of the LMWL, we can conclude that the fog was generated by admixture with advecting moisture. Analysis of covariance ($P < 0.05$) was used to compare differences in slopes between radiation fog and the LMWL. Isotopic characteristics of all meteoric water samples (river, groundwater, rain, fog, and dew) were based on arithmetic means and the associated SDs.

SUPPLEMENTARY MATERIALS

Supplementary material for this article is available at http://advances.sciencemag.org/cgi/content/full/3/3/e1603131/DC1

note S1. Site description.
note S2. Supplementary methods.
note S3. Wind direction and speed measurements.
table S1. Isotopic composition and d-excess of individual precipitation events captured during 2014–2015.
table S2. Isotopic composition and classification of individual fog, dew, groundwater, and river samples captured between 2014 and 2015.
table S3. Monthly rainfall that could have influenced fog and dew formation at the Gobabeb Research and Training Centre during the observation period.
fig. S1. Hybrid Single-Particle Lagrangian Integrated Trajectory model (*60*) of 48-hour backward trajectory analysis of the five precipitation events captured at the Gobabeb Research and Training Centre during the observation period.
References (*61*–*66*)

REFERENCES AND NOTES

1. L. Wang, K. F. Kaseke, M. K. Seely, Effects of non-rainfall water inputs on ecosystem functions. *Wiley Interdiscip. Rev. Water* **4**, e1179 (2017).
2. G. J. Kidron, M. Temina, A. Starinsky, An investigation of the role of water (rain and dew) in controlling the growth form of lichens on cobbles in the Negev Desert. *Geomicrobiol. J.* **28**, 335–346 (2011).
3. L. Wang, P. D'Odorico, L. R. O'Halloran, K. Caylor, S. Macko, Combined effects of soil moisture and nitrogen availability variations on grass productivity in African savannas. *Plant Soil* **328**, 95–108 (2010).
4. R. Brown, A. J. Mills, C. Jack, Non-rainfall moisture inputs in the Knersvlakte: Methodology and preliminary findings. *Water SA* **34**, 275–278 (2008).
5. J. Houston, Groundwater recharge through an alluvial fan in the Atacama Desert, northern Chile: Mechanisms, magnitudes and causes. *Hydrol. Process.* **16**, 3019–3035 (2002).
6. X. Yang, N. Ma, J. Dong, B. Zhu, B. Xu, Z. Ma, J. Liu, Recharge to the inter-dune lakes and Holocene climatic changes in the Badain Jaran Desert, western China. *Quatern. Res.* **73**, 10–19 (2010).
7. F. D. Eckardt, K. Soderberg, L. J. Coop, A. A. Muller, K. J. Vickery, R. D. Grandin, C. Jack, T. S. Kapalanga, J. Henschel, The nature of moisture at Gobabeb, in the central Namib Desert. *J. Arid Environ.* **93**, 7–19 (2013).
8. T. Schröder, M. Javaux, J. Vanderborght, B. Körfgen, H. Vereecken, Implementation of a microscopic soil–root hydraulic conductivity drop function in a three-dimensional soil–root architecture water transport model. *Vadose Zone J.* **8**, 783–792 (2009).
9. R. A. Feddes, H. Hoff, M. Bruen, T. Dawson, P. de Rosnay, P. Dirmeyer, R. B. Jackson, P. Kabat, A. Kleidon, A. Lilly, A. J. Pitman, Modelling root water uptake in hydrological and climate models. *Bull. Am. Meteorol. Soc.* **82**, 2797–2809 (2001).
10. A. Giannini, M. Biasutti, I. M. Held, A. H. Sobel, A global perspective on African climate. *Clim. Change* **90**, 359–383 (2008).
11. D. T. Fischer, C. J. Still, Evaluating patterns of fog water deposition and isotopic composition on the California Channel Islands. *Water Resour. Res.* **43**, W04420 (2007).
12. M. K. Stewart, Stable isotope fractionation due to evaporation and isotopic exchange of falling waterdrops: Applications to atmospheric processes and evaporation of lakes. *J. Geophys. Res.* **80**, 1133–1146 (1975).
13. J. Jouzel, Isotopes in cloud physics: Multiphase and multistage condensation processes, in *Terrestrial Environment, Handbook of Environmental Isotope Geochemistry*, P. Fritz, J. C. Fontes, Eds. (Elsevier, 1986), pp. 61–112.
14. R. Gonfiantini, A. Longinelli, Oxygen isotopic composition of fogs and rains from the North Atlantic. *Experientia* **18**, 222–223 (1962).
15. R. D. Deshpande, A. S. Maurya, B. Kumar, A. Sarkar, S. K. Gupta, Kinetic fractionation of water isotopes during liquid condensation under super-saturated condition. *Geochim. Cosmochim. Acta* **100**, 60–72 (2013).

16. A. Angert, C. D. Cappa, D. J. DePaolo, Kinetic ^{17}O effects in the hydrologic cycle: Indirect evidence and implications. *Geochim. Cosmochim. Acta* **68**, 3487–3495 (2004).
17. F. A. Engelbrecht, J. L. McGregor, C. J. Engelbrecht, Dynamics of the Conformal-Cubic Atmospheric Model projected climate-change signal over southern Africa. *Int. J. Climatol.* **29**, 1013–1033 (2009).
18. M. Hulme, Recent climatic change in the world's drylands. *Geophys. Res. Lett.* **23**, 61–64 (1996).
19. J. R. Henschel, M. K. Seely, Ecophysiology of atmospheric moisture in the Namib Desert. *Atmos. Res.* **87**, 362–368 (2008).
20. W. Dansgaard, Stable isotopes in precipitation. *Tellus* **16**, 436–468 (1964).
21. K. F. Kaseke, L. Wang, H. Wanke, V. Turewicz, P. Koeniger, An analysis of precipitation isotope distributions across Namibia using historical data. *PLOS ONE* **11**, e0154598 (2016).
22. I. Friedman, G. I. Smith, Deuterium content of snow cores from Sierra Nevada area. *Science* **169**, 467–470 (1970).
23. R. Aravena, O. Suzuki, A. Pollastri, Coastal fog and its relation to groundwater in the IV region of northern Chile. *Chem. Geol.* **79**, 83–91 (1989).
24. L. Merlivat, J. Jouzel, Global climatic interpretation of the deuterium-oxygen 18 relationship for precipitation. *J. Geophys. Res.* **84**, 5029–5033 (1979).
25. T. E. Dawson, Fog in the California redwood forest: Ecosystem inputs and use by plants. *Oecologia* **117**, 476–485 (1998).
26. J. R. Gat, E. Matsui, Atmospheric water balance in the Amazon basin: An isotopic evapotranspiration model. *J. Geophys. Res. Atmos.* **96**, 13179–13188 (1991).
27. W. J. Liu, W. Y. Liu, P. J. Li, L. Gao, Y. X. Shen, P. Y. Wang, Y. P. Zhang, H. M. Li, Using stable isotopes to determine sources of fog drip in a tropical seasonal rain forest of Xishuangbanna, SW China. *Agr. Forest Meteorol.* **143**, 80–91 (2007).
28. J. Cui, S. An, Z. Wang, C. Fang, Y. Liu, H. Yang, Z. Xu, S. Liu, Using deuterium excess to determine the sources of high-altitude precipitation: Implications in hydrological relations between sub-alpine forests and alpine meadows. *J. Hydrol.* **373**, 24–33 (2009).
29. X.-F. Wen, X. Lee, X.-M. Sun, J.-L. Wang, Z.-M. Hu, S.-G. Li, G.-R. Yu, Dew water isotopic ratios and their relationships to ecosystem water pools and fluxes in a cropland and a grassland in China. *Oecologia* **168**, 549–561 (2012).
30. A. J. Hill, T. E. Dawson, O. Shelef, S. Rachmilevitch, The role of dew in Negev Desert plants. *Oecologia* **178**, 317–327 (2015).
31. K. Schachtschneider, E. C. February, The relationship between fog, floods, groundwater and tree growth along the lower Kuiseb River in the hyperarid Namib. *J. Arid Environ.* **74**, 1632–1637 (2010).
32. B. Luz, E. Barkan, Variations of $^{17}O/^{16}O$ and $^{18}O/^{16}O$ in meteoric waters. *Geochim. Cosmochim. Acta* **74**, 6276–6286 (2010).
33. J. Jouzel, L. Merlivat, Deuterium and oxygen 18 in precipitation: Modeling of the isotopic effects during snow formation. *J. Geophys. Res. Atmos.* **89**, 11749–11757 (1984).
34. J. R. Petit, J. W. C. White, N. W. Young, J. Jouzel, Y. S. Korotkevich, Deuterium excess in recent Antarctic snow. *J. Geophys. Res. Atmos.* **96**, 5113–5122 (1991).
35. L. Wang, K. K. Caylor, J. C. Villegas, G. A. Barron-Gafford, D. D. Breshears, T. E. Huxman, Partitioning evapotranspiration across gradients of woody plant cover: Assessment of a stable isotope technique. *Geophys. Res. Lett.* **37**, L09401 (2010).
36. L. Wang, S. P. Good, K. K. Caylor, L. A. Cernusak, Direct quantification of leaf transpiration isotopic composition. *Agric. For. Meteorol.* **154–155**, 127–135 (2012).
37. K. J. Esler, P. W. Rundel, P. Vorster, Biogeography of prostrate-leaved geophytes in semi-arid South Africa: Hypotheses on functionality. *Plant Ecol.* **142**, 105–120 (1999).
38. M. Ebner, T. Miranda, A. Roth-Nebelsick, Efficient fog harvesting by *Stipagrostis sabulicola* (Namib dune bushman grass). *J. Arid Environ.* **75**, 524–531 (2011).
39. A. Roth-Nebelsick, M. Ebner, T. Miranda, V. Gottschalk, D. Voigt, S. Gorb, T. Stegmaier, J. Sarsour, M. Linke, W. Konrad, Leaf surface structures enable the endemic Namib desert grass *Stipagrostis sabulicola* to irrigate itself with fog water. *J. R. Soc. Interface* **9**, 1965–1974 (2012).
40. P. Foster, The potential negative impacts of global climate change on tropical montane cloud forests. *Earth Sci. Rev.* **55**, 73–106 (2001).
41. G. J. Kidron, A. Starinsky, D. H. Yaalon, Cyanobacteria are confined to dewless habitats within a dew desert: Implications for past and future climate change for lithic microorganisms. *J. Hydrol.* **519**, 3606–3614 (2014).
42. L. Wang, K. Caylor, D. Dragoni, On the calibration of continuous, high-precision $\delta^{18}O$ and $\delta^{2}H$ measurements using an off-axis integrated cavity output spectrometer. *Rapid Commun. Mass Spectrom.* **23**, 530–536 (2009).
43. C. Tian, L. Wang, K. A. Novick, Water vapor $\delta^{2}H$, $\delta^{18}O$ and $\delta^{17}O$ measurements using an off-axis integrated cavity output spectrometer – Sensitivity to water vapor concentration, delta value and averaging-time. *Rapid Commun. Mass Spectrom.* **30**, 2077–2086 (2016).
44. M. F. Miller, Isotopic fractionation and the quantification of ^{17}O anomalies in the oxygen three-isotope system: An appraisal and geochemical significance. *Geochim. Cosmochim. Acta* **66**, 1881–1889 (2002).
45. B. Luz, E. Barkan, The isotopic ratios $^{17}O/^{16}O$ and $^{18}O/^{16}O$ in molecular oxygen and their significance in biogeochemistry. *Geochim. Cosmochim. Acta* **69**, 1099–1110 (2005).
46. J. R. Hulston, H. G. Thode, Variations in the S^{33}, S^{34}, and S^{36} contents of meteorites and their relation to chemical and nuclear effects. *J. Geophys. Res.* **70**, 3475–3484 (1965).
47. X. Lu, L. Wang, M. Pan, K. F. Kaseke, B. Li, A multi-scale analysis of Namibian rainfall over the recent decade – Comparing TMPA satellite estimates and ground observations. *J. Hydrol.* **8**, 59–68 (2016).
48. M. Majoube, Oxygen-18 and deuterium fractionation between water and steam. *J. Chim. Phys. Phys. Chim. Biol.* **68**, 1423–1436 (1971).
49. J. Olivier, Spatial distribution of fog in the Namib. *J. Arid Environ.* **29**, 129–138 (1995).
50. K. F. Kaseke, A. J. Mills, K. Esler, J. Henschel, M. K. Seely, R. Brown, Spatial variation of "non-rainfall" water input and the effect of mechanical soil crusts on input and evaporation. *Pure Appl. Geophys.* **169**, 2217–2229 (2012).
51. B. R. Scanlon, Evaluation of methods of estimating recharge in semiarid and arid regions in the Southwestern U.S., in *Groundwater Recharge in a Desert Environment: The Southwestern United States*, J. F. Hogan, F. M. Phillips, B. R. Scanlon, Eds. (American Geophysical Union, 2004), pp. 235–354.
52. K. Mizuno, Environmental change and vegetation succession along an ephemeral river: The Kuiseb in the Namib Desert. *Afr. Stud. Monogr.* **40**, 3–18 (2010).
53. W. J. Shuttleworth, J. H. C. Gash, C. R. Lloyd, C. J. Moore, J. Roberts, A. D. O. M. Filho, G. Fisch, V. De Paula Silva Filho, M. D. N. G. Ribeiro, L. C. B. Molion, L. D. De Abreu Sá, J. C. A. Nobre, O. M. R. Cabral, S. R. Patel, J. C. De Moraes, Eddy correlation measurements of energy partition for Amazonian forest. *Q. J. Roy. Meteorol. Soc.* **110**, 1143–1162 (1984).
54. E. Salati, A. Dall'Olio, E. Matsui, J. R. Gat, Recycling of water in the Amazon basin: An isotopic study. *Water Resour. Res.* **15**, 1250–1258 (1979).
55. L. Wang, S. P. Good, K. K. Caylor, Global synthesis of vegetation control on evapotranspiration partitioning. *Geophys. Res. Lett.* **41**, 6753–6757 (2014).
56. S. Jasechko, Z. D. Sharp, J. J. Gibson, S. J. Birks, Yi Y., P. J. Fawcett, Terrestrial water fluxes dominated by transpiration. *Nature* **496**, 347–350 (2013).
57. D. Yakir, L. da S. L. Sternberg, The use of stable isotopes to study ecosystem gas exchange. *Oecologia* **123**, 297–311 (2000).
58. H. Craig, Isotopic composition and origin of the Red Sea and Salton Sea geothermal brines. *Science* **154**, 1544–1548 (1966).
59. L. Araguás-Araguás, K. Froehlich, K. Rozanski, Deuterium and oxygen-18 isotope composition of precipitation and atmospheric moisture. *Hydrol. Process.* **14**, 1341–1355 (2000).
60. A. F. Stein, R. R. Draxler, G. D. Rolph, B. J. B. Stunder, M. D. Cohen, F. Ngan, NOAA's HYSPLIT atmospheric transport and dispersion modeling system. *Bull. Am. Meteorol. Soc.* **96**, 2059–2077 (2015).
61. P. J. Jacobson, K. M. Jacobson, M. K. Seely, *Ephemeral Rivers and their Catchments: Sustaining People and Development in Western Namibia* (Desert Research Foundation of Namibia, Windhoek, 1995).
62. O. Dahan, B. Tatarsky, Y. Enzel, C. Kulls, M. Seely, G. Benito, Dynamics of flood water infiltration and ground water recharge in hyperarid desert. *Groundwater* **46**, 450–461 (2008).
63. A. Burke, Savanna trees in Namibia—Factors controlling their distribution at the arid end of the spectrum. *Flora* **201**, 189–201 (2006).
64. J. Lange, Dynamics of transmission losses in a large and stream channel. *J. Hydrol.* **306**, 112–126 (2005).
65. R. S. Schemenauer, P. Cereceda, A proposed standard fog collector for use in high-elevation regions. *J. Appl. Meteorol.* **33**, 1313–1322 (1994).
66. J. L. Monteith, Dew. *Q. J. R. Meteorol. Soc.* **83**, 322–341 (1957).

Acknowledgments: We would like to acknowledge R. Gottlieb, N. Kandali, T. Wassenaar, and R. Mushi for the logistical support and fieldwork assistance rendered under the auspices of the Gobabeb Research and Training Centre. We thank the Gobabeb Research and Training Centre for the meteorological data (wind speed and direction). We thank K. Mandernack, two anonymous reviewers, and P. Bierman for providing valuable comments to improve the quality of this manuscript. **Funding:** Funding for this work was made available from the NSF (IIA-1427642 and EAR-1554894) to L.W. **Author contributions:** K.F.K. and L.W. conceived the study and performed the experiment. K.F.K. analyzed the data. K.F.K. and L.W. wrote the manuscript with substantial input from M.K.S. **Competing interests:** The authors declare that they have no competing interests. **Data and materials availability:** All data needed to evaluate the conclusions in the paper are present in the paper and/or the Supplementary Materials. Additional data related to this paper may be requested from the authors.

Submitted 9 December 2016
Accepted 9 February 2017
Published 22 March 2017
10.1126/sciadv.1603131

Citation: K. F. Kaseke, L. Wang, M. K. Seely, Nonrainfall water origins and formation mechanisms. *Sci. Adv.* **3**, e1603131 (2017).

Science Advances
AAAS

Nonrainfall water origins and formation mechanisms
Kudzai Farai Kaseke, Lixin Wang and Mary K. Seely (March 22, 2017)
Sci Adv 2017, 3:.
doi: 10.1126/sciadv.1603131